

Physical properties of Cr₇₈Al₂₂ thin films

ARE Prinsloo¹, CJ Sheppard¹, HA Derrett¹, N van den Berg² and EE Fullerton³

¹Department of Physics, University of Johannesburg, PO Box 524, Auckland Park, 2006, South Africa

²Department of Physics, University of Pretoria, Private bag X20, Hatfield, 0028, South Africa

³Center for Magnetic Recording Research, University of California, San Diego, 9500 Gilman Dr, La Jolla, CA 92093-0401, USA

Author e-mail address: alettap@uj.ac.za

Abstract. The Cr_{100-x}Al_x alloy system shows astonishing behaviour at higher Al concentrations [1]. Very high Néel temperatures ($T_N > 800$ K) are observed in samples with $x > 20$. The SDW amplitude for these alloys has a value of about $1\mu_B$ – larger than in other Cr alloy systems. In addition both the Hall coefficient and the resistivity for samples in the concentration range $15 \leq x \leq 25$ are large. In this concentration range the resistivity has a negative temperature dependence and is in form characteristic of narrow-bandgap semiconductors. Combining these unique bulk characteristics with exceptional thin film properties seen for Cr and its alloys, appears to be a way forward in order to improve modern technologies, such as used in data storage. For this reason the present study focus on Cr₇₈Al₂₂ thin films in a thickness (t) range 12 to 400 nm, prepared on MgO(100), MgO(110), a-plane sapphire and quartz substrates, deposited using DC magnetron sputtering. AFM results on the fused silica samples indicate interesting growth patterns with cubic structures forming in the thicker samples. This is supported by XRD results indicating that for the samples prepared on fused silica substrates preferred Cr(110) growth occurs for $t \geq 100$ nm. XRD results also show good epitaxial growth of the films prepared on the MgO and a-plane sapphire substrates. Resistance (R) as function of temperature (T) investigations were done using the standard four-point probe method in a temperature range 77 K $< T < 400$ K and show negative temperature dependence. Interestingly, the behaviour of $R(T)$ differs for those samples prepared on MgO(100), as the film with $t = 400$ nm shows characteristics not associated with narrow-bandgap semiconductors.

1. Introduction

The richness of magnetic phenomena of Cr and Cr alloys has attracted considerable interest for many years [1]. Bulk Cr is an itinerant electron antiferromagnetic material that forms an incommensurate (I) spin density wave (SDW) phase below its Néel temperature $T_N = 311$ K [1]. The ISDW period varies from 78 Å at T_N to 60 Å at 10 K [2, 3]. Thin films and hetero-structures of Cr and Cr alloys show fascinating properties, not observed in the bulk [3, 4]. These properties include dimensionality, surface and proximity effects, as well as the mediating role of Cr thin films in exchange coupled super-lattices and in giant magneto-resistive (GMR) materials [2].

The Cr_{100-x}Al_x alloy system has shown interesting behaviour recently explored further [5] around the triple point where the commensurate SDW (CSDW), ISDW and paramagnetic phases co-exist [1]. The

study on $\text{Cr}_{100-x}\text{Al}_x$ single crystals [5] is considered a detailed investigation of the magnetic behaviour of Cr alloy systems in the proximity of the triple point concentration on the concentration-temperature magnetic phase diagram. The data indicates that the triple point minimum on this diagram seen at $x \approx 2.3$ might be deeper and much narrower than previously thought, resembling quantum critical behaviour at this point. However, at higher Al concentrations new and astonishing behaviour begin to emerge [1]. Very high Néel temperatures ($T_N > 800$ K) are observed in samples with $x > 20$. The SDW amplitude for these alloys has a value of about $1\mu_B$ – larger than in other Cr alloy systems. In addition both the Hall coefficient and the resistivity for samples in the concentration range $15 \leq x \leq 25$ is large [1]. In this concentration range the resistivity of bulk samples have a negative temperature dependence and has a similar behaviour as that of narrow-gap semiconductors [1].

Combining these unique bulk characteristics of Cr-Al with exceptional thin film properties seen for Cr and its alloys [2], appears to be a way forward in order to extend the understanding of the behaviour of the SDW in this system and also provides basic information that can possibly improve modern technologies in future, such as those applicable to data storage. This paper focuses on the structural, surface and electrical properties of epitaxial and polycrystalline $\text{Cr}_{78}\text{Al}_{22}$ thin films in a thickness (t) range 12.5 to 400 nm.

2. Experimental

The Cr-Al thin films were deposited using Direct-Current (DC) magnetron sputtering at a substrate temperature of 973 K and argon working pressure of 3 mTorr. The Cr and Al were co-sputtered from elemental sources onto single-crystal MgO(110), MgO(100), a-plane sapphire, and amorphous quartz substrates. The Al-concentration in the Cr-Al films was obtained by adjusting the Al target deposition power. The samples were prepared at a fixed concentration of Cr + 22 at.% Al with thicknesses varying from 12 to 400 nm. Atomic force microscopy (AFM) imaging was used to study the topographic properties of the $\text{Cr}_{78}\text{Al}_{22}$ thin films and the film structure was characterized using X-ray diffraction (XRD) techniques. Electrical resistance measurements using standard DC four-probe method from 77 to 400 K were employed to investigate the electrical transport properties of these samples.

3. Results

The XRD measurements indicate that all the films prepared on MgO(100), MgO(110) and a-plane sapphire, are epitaxial and exhibit a single crystallographic orientation, with the Cr-Al showing preferred growth directions of (100), (211) and (110) for the respective substrates. The samples prepared on quartz were polycrystalline for thicknesses $12.5 \text{ nm} < t < 100 \text{ nm}$ and $t = 400 \text{ nm}$, however for thickness $t = 100$ and 200 nm preferred Cr(110) growth orientation is shown. Examples of XRD measurements for the samples are shown in Figs. 1 (a), (b), (c) and (d) for the various substrates.

The full-width at half-maximum (FWHM) of the Bragg peaks was used to determine the length scale (in growth direction) over which the film is structurally coherent [6]. The Debye-Scherrer formula was used to calculate the coherence lengths after removing the instrument resolution. For $\text{Cr}_{78}\text{Al}_{22}$ thin films ($12 \leq t \leq 400 \text{ nm}$) grown on MgO(100) substrates the crystal coherence length in growth directions (100) of the films increased with increasing t reaching a maximum at $t = 100 \text{ nm}$ thereafter it decreases and levels off at approximately 13.5 nm for $t \geq 200 \text{ nm}$. For the MgO(110) substrates the crystal coherence length in growth directions (110) generally increased with increasing t . Samples prepared on a-plane sapphire show an increase in coherence length with increase in sample thickness reaching a maximum for a 100 nm sample and then the coherence length decreased again. Results obtained for the $\text{Cr}_{78}\text{Al}_{22}$ thickness series are summarized in Table 1.

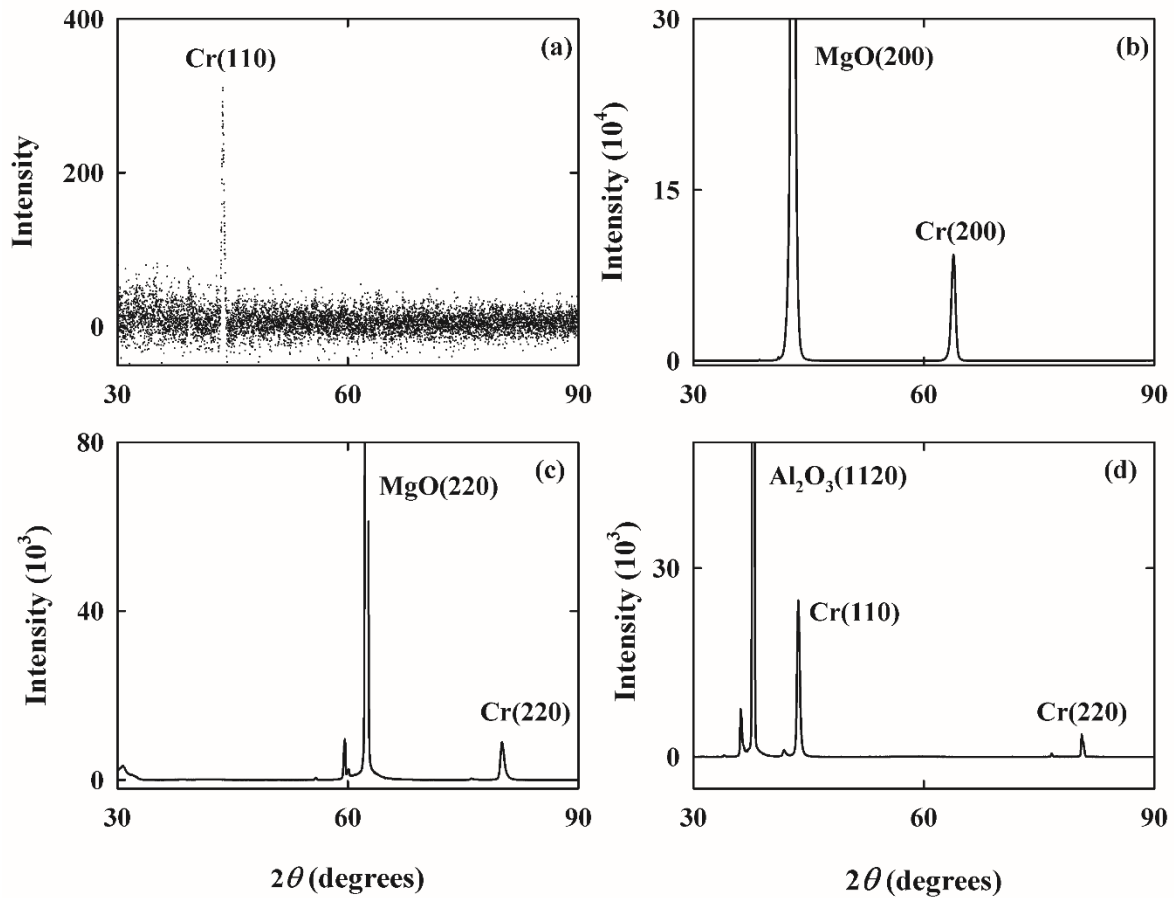


Figure 1. θ - 2θ XRD scans, with the scattering vector normal to the plane of the film, for the $\text{Cr}_{78}\text{Al}_{22}$ thin films prepared on (a) quartz ($t = 200$ nm); (b) MgO(100) ($t = 100$ nm), (c) MgO(110) ($t = 200$ nm) and (d) a-plane sapphire ($t = 50$ nm) substrates.

t (nm)	MgO(100)			MgO(110)			a-plane sapphire		
	FWHM (200)	T_{coh} (nm)	Mosaic (200)	FWHM (211)	T_{coh} (nm)	Mosaic (211)	FWHM (110)	T_{coh} (nm)	Mosaic (110)
12.5	1.98°	8.3	1.18°	1.15°	9.5	0.89°	0.66°	13.5	0.28°
25	1.64°	11.5	0.85°	0.84°	12.9	1.47°	0.45°	19.1	0.56°
50	1.32°	15.9	0.61°	0.73°	14.9	1.18°	0.40°	22.4	0.46°
100	0.97°	16.0	0.61°	0.75°	14.6	1.06°	0.37°	24.2	0.42°
200	1.16°	13.6	1.16°	0.57°	19.0	0.50°	0.40°	22.2	0.39°
400	0.72°	13.6	0.72°	0.60°	18.0	0.70°	0.43°	21.0	0.46°

Table 1. The measured out-of-plane full-width at half-maximum (FWHM) XRD parameters of the selected Bragg peaks and the mosaic spread of this peak, for epitaxial $\text{Cr}_{78}\text{Al}_{22}$ films of thickness t prepared at 800°C on MgO(100), MgO(110) and a-plane sapphire substrates, respectively. The coherence length, T_{coh} , was calculated using the Debye-Scherrer equation after removing the resolution of the instrument.

The mosaic spread was determined from the FWHM of the rocking curve [6]. For $\text{Cr}_{78}\text{Al}_{22}$ thin films prepared on $\text{MgO}(100)$ substrates (Table 1) the general tendency is a decrease in the mosaicity with increase in t , except for the film of thickness 200 nm that does not fit into this pattern, with a mosaicity of 1.16° . This indicates a general trend of improved crystal quality with films thickness, but since the values exceeds 0.5° there is not a high degree of crystallographic alignment in these samples [6, 7] which is typical for Cr and Cr alloys epitaxially grown onto MgO. No clear tendency is seen in the mosaicity of the thickness series prepared on $\text{MgO}(110)$. The films prepared on the a-plane sapphire however, had a high degree of crystallographic alignment with the mosaicities less than 0.5° , except for the 35 nm sample with a mosaicity of 0.56° .

AFM studies on the $\text{Cr}_{78}\text{Al}_{22}$ monolayers thickness series indicate that polycrystalline film with $t = 12.5$ nm has a relatively smooth surface morphology, depicted in figure 2 (a). As t increases, grains become more visible in the AFM images accompanied by an increase in surface roughness. For the sample with $t = 200$ nm clear cubic crystals are visible (depicted in figure 2 (b)). Interestingly this sample also showed preferred $\text{Cr}(110)$ growth. On increasing the thickness to $t > 200$ nm columnar growth observed, with a clear increase in surface roughness. Figure 2 (c) show the AFM image for the epitaxial film with $t = 100$ nm prepared on $\text{MgO}(110)$ and columnar structures consisting of merged cubical units are observed. However, for the samples prepared on a-plane sapphire the surface appears relatively smooth with no columnar structures (as an example consider figure 2 (d) for the sample with

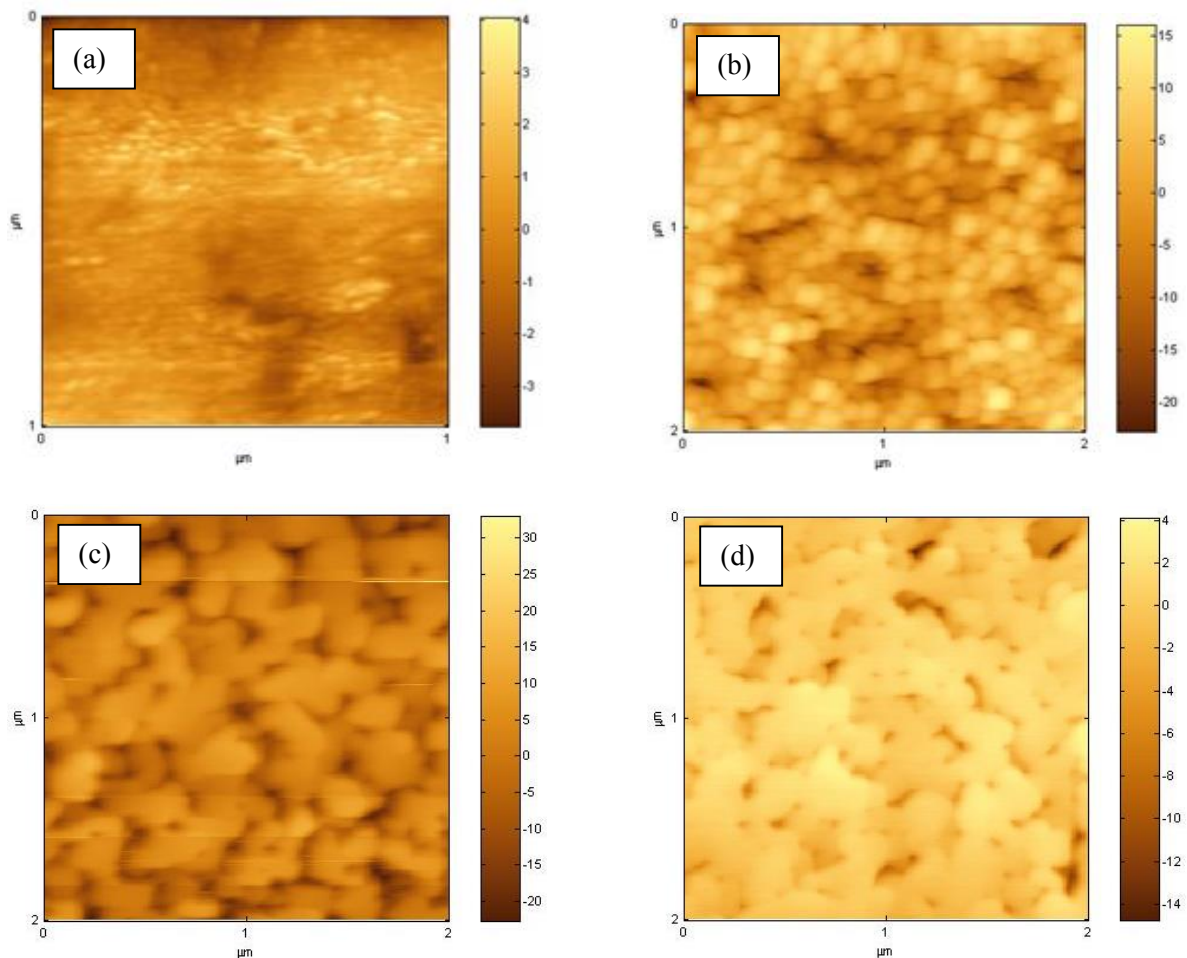


Figure 2. AFM images for $\text{Cr}_{78}\text{Al}_{22}$ thin films prepared on (a) quartz ($t = 12.5$ nm); (b) quartz ($t = 200$ nm); (c) $\text{MgO}(110)$ ($t = 100$ nm) and (d) a-plane sapphire ($t = 400$ nm). The height range (in nm) are indicated to the right of each figure.

thickness 400 nm prepared on a-plane sapphire). This corresponds with the low mosaicity and high crystallinity of the samples prepared on a-plane sapphire reported from the XRD results for this thickness series.

The electrical resistance (R) as a function of temperature (T) measurements were used to electrically characterise the samples. T_N could not be determined for the samples investigated as the transition from antiferromagnetic to paramagnetic phase it is expected to occur at $T > 800$ K for this Al concentration. The $R - T$ curves of the samples prepared on quartz and MgO(110) show negative gradients in the temperature regions investigated, indicative of narrow-band semiconductor behaviour – as was also observed for bulk $\text{Cr}_{78}\text{Al}_{22}$ [1]. Representative curves are shown in figure 3 for the samples prepared on (a) quartz ($t = 25$ nm) and (b) MgO(110) ($t = 50$ nm). Although only representative data are shown figure 3, all the samples in each series were characterized and results indicate that resistance decreases with increase in layer thickness as can be expected. The $R - T$ behaviour of the thickness series prepared on MgO(100) however show a changing behaviour as the thickness is varied. Figures 3 (c) and (d) shows the behaviour for the $\text{Cr}_{78}\text{Al}_{22}$ thin film samples prepared on MgO(100) with thicknesses 50 nm and 400 nm, respectively. Over this series the negative gradient observed for the thinner samples gradually makes way for a clear change in gradient in the $R - T$ curve from $dR/dT > 0$ to $dR/dT < 0$ at a temperature of approximately 230 K. Interestingly, this implies that the structural and dimensionality effects in the thin film samples prepared on MgO(100) resulted in new characteristics different from the semiconductor behaviour observed in bulk samples of this concentration.

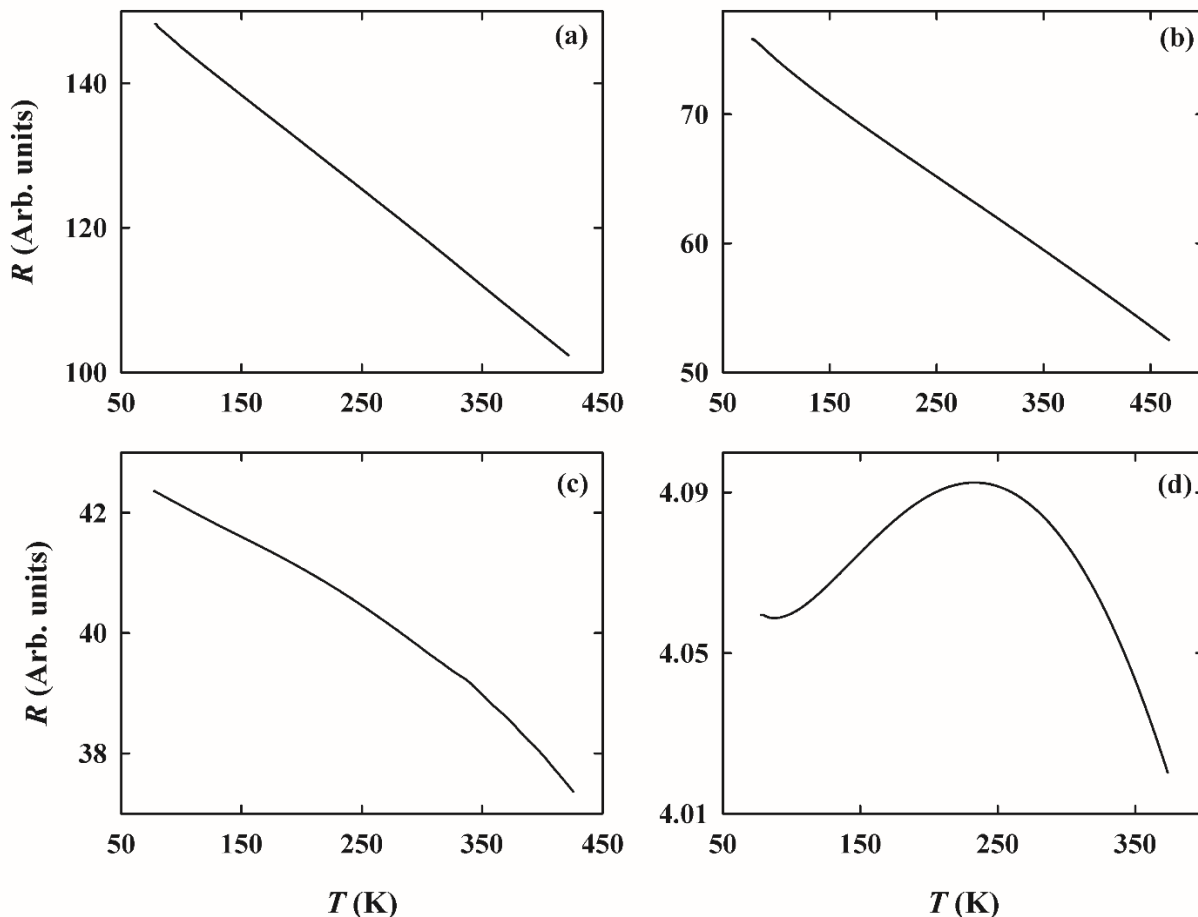


Figure 3. Resistance (R) versus temperature (T) graphs for a $\text{Cr}_{78}\text{Al}_{22}$ thin films prepared on (a) quartz ($t = 25$ nm); (b) MgO(110) ($t = 50$ nm); (c) MgO(100) ($t = 50$ nm) and (d) MgO(100) ($t = 400$ nm).

4. Conclusions

The results show clear difference between films depending on substrate and film thickness, both in the structure and transport properties. For the $\text{Cr}_{78}\text{Al}_{22}$ thickness series prepared on $\text{MgO}(110)$ XRD results indicated a general decrease in mosaicity and an increase in coherence length with increase in the layer thickness. Narrow bandgap semiconductor behaviour was inferred to from the $R - T$ measurements for the samples prepared on $\text{MgO}(110)$ and quartz. The series prepared on a-plane sapphire showed high crystallinity with optimal coherence length at $t = 100$ nm. Preliminary AFM studies show that the films prepared on the a-plane sapphire was more smooth than those prepared on $\text{MgO}(110)$ that show more columnar growth.

All the samples in the $\text{Cr}_{78}\text{Al}_{22}$ thickness series on quartz also showed narrow bandgap semiconductor behaviour in the temperature range studied. AFM studies showed that the smooth surface of the thin samples is gradually replaced by bigger grain structures and an increase in the surface roughness. Cubic crystallites are observed at $t = 200$ nm, followed by columnar growth seen in the sample with $t = 400$ nm. The XRD and AFM results for this series is complementary.

For the $\text{Cr}_{78}\text{Al}_{22}$ thickness series prepared on $\text{MgO}(100)$ a general decrease in mosaicity with increase in layer thickness is observed, with the coherence length of the samples optimal at a thickness of 100 nm. The electrical characteristics of this sample series gradually changed with layer thickness, and the $R - T$ semiconductor behaviour disappeared in the thickest film for temperatures below approximately 230 K.

More work is required to fully understand the complex dimensionality effects behaviour seen in the $\text{Cr}_{78}\text{Al}_{22}$ thickness series prepared on $\text{MgO}(100)$. In order to do so it is suggested that the sample series be extended to include more samples with different sample thicknesses so that strong correlations can be drawn between the morphological, structural and electrical properties of these thin films.

5. Acknowledgement

The authors wish to thank the National Research Funding of South Africa for financial support towards this study (Grant number 80928; 80631 and 93551) and the financial contributions from Faculty of Science from the University of Johannesburg is also acknowledged.

References

- [1] Fawcett E, Alberts HL, Galkin VY, Noakes DR, Yakhmi JV 1994 *Rev. Mod. Phys.* **66** 25
- [2] Zabel HJ, *J. Phys.: Condens. Matter* **11** (1999) 9303
- [3] Fullerton EE, Robertson JL, Prinsloo AER, Alberts HL, Bader SD 2003 *Phys. Rev. Lett.* **91** 237201
- [4] Kummamuru RK, Soh YA 2008 *Nature* **452** 859
- [5] Sheppard CJ, Prinsloo ARE, Alberts HL, Muchono B and Strydom AM 2014 *J. Alloys Compd.* **595** 164
- [6] Mattson JE, Fullerton EE, Sowers CH, Bader SD 1995 *J. Vac. Sci. Technol.* **A13** (2) 276
- [7] Mattson JE, Brunnitt B, Brodsky MB, Ketterson JB 1990 *J. Appl. Phys.* **67** (9) 4889